4682–4696 *Nucleic Acids Research, 2014, Vol. 42, No. 7* *Published online 1 February 2014*
doi:10.1093/nar/gku098

Curli synthesis and biofilm formation in enteric bacteria are controlled by a dynamic small RNA module made up of a pseudoknot assisted by an RNA chaperone

Valérie Bordeau and Brice Felden*

Biochimie Pharmaceutique, Rennes University, Inserm U835-UPRES EA2311, 2 avenue du Prof. Léon, Bernard, 35043 Rennes, France

Received December 6, 2013; Revised January 7, 2014; Accepted January 10, 2014

ABSTRACT

RydC pseudoknot aided by Hfq is a dynamic regulatory module. We report that RydC reduces expression of curli-specific *gene D* transcription factor required for adhesion and biofilm production in enterobacteria. During curli formation, *csgD* messenger RNA (mRNA) synthesis increases when endogenous levels of RydC are lacking. In *Escherichia coli* and *Salmonella enterica*, stimulation of RydC expression also reduces biofilm formation by impairing curli synthesis. Inducing RydC early on in growth lowers CsgA, -B and -D protein and mRNA levels. RydC's 5′-domain interacts with *csgD* mRNA translation initiation signals to prevent initiation. Translation inhibition occurs by an antisense mechanism, blocking the translation initiation signals through pairing, and that mechanism is facilitated by Hfq. Although Hfq represses *csgD* mRNA translation without a small RNA (sRNA), it forms a ternary complex with RydC and facilitates pseudoknot unfolding to interact with the *csgD* mRNA translation initiation signals. RydC action implies Hfq-assisted unfolding and mRNA rearrangements, but once the pseudoknot is disrupted, Hfq is unnecessary for regulation. RydC is the sixth sRNA that negatively controls CsgD synthesis. Hfq induces structural changes in the mRNA domains targeted by these six sRNAs. What we describe is an ingenious process whereby pseudoknot opening is orchestrated by a chaperone to allow RNA control of gene expression.

INTRODUCTION

Many bacterial small RNAs (sRNAs) modulate gene expression by base pairing with target messenger RNAs (mRNAs) (1). *Trans*-encoded sRNAs regulate mRNA expression through small discontinuous 'seed-pairings', which are usually at or near the translation initiation signals (TIS) of their targets, whereas *cis*-antisense sRNAs are encoded on the DNA strand opposite to that of their targets (2). In the cellular transcript overflow, each of these base-pairing sRNAs has to efficiently locate and bind to its mRNA target, recognizing these through high-affinity contacts made by a few accessible nucleotides. These are usually situated in single strands (i.e. C-rich stretches), in loops of the regulator, in the targets or in both places. After this primary interaction, the structure of the two RNAs is generally rearranged and additional base pairs are formed. In gram-negative bacteria, the Hfq RNA-binding protein is usually required for *trans*-encoded sRNA stability and operation (2). Hfq facilitates sRNA–mRNA base pairing by binding both RNAs simultaneously and/or by changing one or both of the RNA structures (3), but its exact contribution at a molecular level remains, for the most part, unresolved.

RydC is a *trans*-encoded sRNA expressed by enteric bacteria that folds as a pseudoknot and interacts with Hfq, a protein that positively influences sRNA stability *in vivo* (4). In *Escherichia coli*, RydC controls *yejABEF* mRNA expression producing an inner membrane ATP Binding Cassette (ABC) transporter (4). The *yej*ABEF allows the uptake of translation inhibitor microcin C, a peptide-nucleotide antibiotic targeting aspartyl-tRNA (transfer RNA) synthetase (5). In *Salmonella*, the *yej* operon is involved in virulence, interferes with Major Histocompatibility Complex (MHC) I presentation, counteracts antimicrobial peptides and provides a nutritious peptide source for survival and proliferation inside the host (6). In intracellular *Salmonella typhimurium*, RydC expression is repressed (7), and perhaps, as is the case for *E. coli,* this is to reduce nutrient uptake by lowering *yej* mRNA levels (4). In *Salmonella*, RydC selectively activates

*To whom correspondence should be addressed. Tel: +33 223234851; Fax: +33 223234456; Email: bfelden@univ-rennes1.fr

the longer isoform of the cyclopropane fatty acid (CFA) synthase mRNA to regulate membrane stability (8).

Here, we report that RydC negatively controls curli and biofilm production in both *E. coli* and *Salmonella enterica*. Many bacteria switch between a single-cell motile lifestyle and multicellular sessile adhesive states forming biofilm, resulting in a protected growth mode that allows cells to survive and thrive in hostile environments (9). Biofilm formation is a complex process involving numerous sensory signals linked to elaborate gene regulations via a transcription factor array. When enteric bacteria construct biofilms, they involve curli-specific genes (*csg*) organized in the *csgDEFG* and *csgBAC* bicistronic operon. *csgEFG* is required for export, and CsgD is a member of the LuxR family of transcriptional regulators that activate *csgBA* to synthesize the structural components of curli fimbriae. CsgD governs the synthesis of the extracellular matrix components cellulose and curli fimbriae in enteric bacteria responsible for the 'rdar' morphotype (10). A collection of environmental alerts adjust CsgD expression, causing it to swap from a mobile to an attached mode (11). The *csgD* promoter is positively regulated by several transcription factors (11) and by small signalling molecules (12), whereas its expression is negatively controlled at the post-transcriptional level by five sRNAs acting in collaboration with Hfq. In response to various environmental signals, OmrA/B (13), McaS (14), RprA (15) and GcvB (16) all downregulate CsgD translation by binding at specific locations onto the *csgD* mRNA 5′-untranslated region (UTR), which is a signal perception platform (17).

Experimental evidence provided in this report shows that RydC, with the help of Hfq, negatively controls *csgD* mRNA and protein levels. It diminishes *csgA* and *csgBA* mRNA and protein levels as well, thus attenuating curli synthesis and biofilm production. CsgD regulation by RydC occurs by direct pairing at the *csgD* mRNA TIS, preventing translation initiation. On complex formation with the *csgD* mRNA, probing and mutational data indicate that RydC induces a structural rearrangement of the *csgD* mRNA TIS, and the sRNA pseudoknot partially unfolds its 5′-domain to pair with its mRNA target. In the absence of sRNA, Hfq acts as a repressor of *csgD* mRNA translation, but it promotes complex formation between the two RNAs, presumably by facilitating pseudoknot opening to increase accessibility to the RydC 5′-domain. This makes RydC the sixth sRNA to negatively influence the expression of the csgD transcription factor that regulates collective behaviour in enteric bacteria, determining progression from a planktonic to a sessile condition.

MATERIALS AND METHODS

Bacterial strains, media and growth conditions

Escherichia coli K-12 MG1655Z1, *Shigella sonnei* and *S. enterica* strains and their derivatives were used (Supplementary Table S1). *RydC* gene disruption and overexpression in *E. coli* cells were done as previously described (4). The biofilm assays were performed in 96-well polystyrene plates, as previously described (18). *E. coli*, *S. enterica* and *S. sonnei* cells were grown aerobically under static conditions at 28°C in half-diluted M9 media supplemented with a 0.4% glucose carbon source. After 48-h growth, planktonic cells were discarded and kept for growth evaluation at $OD_{600\,nm}$. Each well was washed twice with phosphate-buffered saline and put into a 'swimming pool', pooled with the initial supernatant. Biofilm was developed in plates then dyed with crystal violet for 15 min at room temperature. The biofilm was recovered through application of an 80% absolute ethanol and 20% acetone solution and by pipetting up and down. After two further washes in 'ethanol/acetone', the number of surface-attached bacteria was estimated from the optical density at 590 nm and divided by the evaluation of growth at 600 nm. Curli expression was monitored for 48 h at 28°C on Congo red plates (1% casamino acids, 0.1% yeast extract, 20 μg/ml Congo red and 10 μg/ml Coomassie brilliant blue G). Expression of csg proteins and *csg* genes was accomplished by growing cells on YESCA agar (1% casamino acids, 0.1% yeast extract and 2% agar) at 28°C and for various time frames. When required, the growth media were supplemented with spectinomycin (10 μg/ml) or ampicillin (50 μg/ml).

Northern blots and quantitative RT-PCR experiments

After 8-, 10-, 15-, 24- and 48-h incubation at 28°C on YESCA plates, cells were scraped with fresh ethanol containing 5% phenol and immediately centrifuged for 10 min at 4500 rpm at 4°C. Total RNA extraction was performed on the cell pellet by the hot acid phenol method as described previously (4). For *csgD* and *csgA* mRNA analysis, 20 μg total RNA was fractionated by 1% agarose gel containing 2.2 M formaldehyde, then transferred onto nylon membranes (Zeta-Probe GT, Bio-Rad) using a Vacuum Blotter (Bio-Rad) as per the manufacturer's protocol. For RydC analysis, northern blot analysis was carried out by loading 10 μg total RNA/lane onto a 5% PAGE containing 8 M urea. The gel was then electroblotted in 0.5× Tris-HCl, Borate, EDTA (TBE) onto nylon membrane (Zeta-Probe GT) at 30 V for 1 h 30 min. Prehybridization and hybridization were performed in ExpressHyb (Clontech). *CsgD* mRNA, *csgA* mRNA, RydC, transfer-messenger RNA (tmRNA) and 5S ribosomal RNA (rRNA) were analysed using 5′-end-labelled DNA oligonucleotides (Supplementary Table S2). Signals were detected using a PhosphorImager and quantified using ImageQuant NT 5.2 (both from Molecular Dynamics). *CsgD* mRNA and RydC expression levels in the *E. coli* strains were monitored by quantitative PCR. After an overnight culture in YESCA broth and then incubations for 2, 4 and 8 h on YESCA plates at 28°C, total RNA were extracted as described for the northern blots. The complementary DNAs (cDNAs) were produced using a High-Capacity cDNA Reverse Transcription Kit (Applied Biosystems). RT-PCR was performed using RealMasterMIX SYBR kit (5′PRIME) on a StepOnePlus Real-Time PCR (Applied Biosytems). Using the comparative ΔΔCt

method, the amount of *csgD* mRNA was normalized against the *tmrna* reference gene.

Western blots

After 8-, 10-, 15-, 24- and 48-h incubation at 28°C on YESCA plates, cells were scraped with phosphate-buffered saline and immediately centrifuged for 10 min at 4500 rpm at 4°C. Cell pellets were then treated with formic acid in ice during 5 min. After evaporation in Speedvac, each pellet was dissolved in sample loading buffer (Laemmli 1X with 10% ß-mercaptoethanol) and heated at 90°C for 5 min. Samples were separated onto 15% SDS–PAGE gels and transferred to PolyVinyliDene Fluoride (PVDF) membranes (GE Healthcare) at 100 V for 1 h. Membranes were blocked in TBS containing 5% milk. Incubation with primary antibodies was performed for 2 h at room temperature at a 1:1000 dilution for anti-CsgA and at 1:5000 for anti-CsgD. After the incubation with the secondary antibody for 2 h at room temperature, the blots were washed in Tris-Buffered Saline (TBS) containing 0.05% Tween and then developed in ECL Western Blotting Detection Reagent (GE Healthcare). Results were obtained by exposing the blots with an ImageQuant LAS 4000 (GE Healthcare) for incremental incubation times. The signals were quantified using Image-Quant NT 5.2.

In vitro transcription, purification and end labelling

To generate the various *csgD* mRNA fragments as well as the sRNA's RydC, DNA templates containing a T7 promoter sequence were generated by PCR using the appropriate primers (Supplementary Table S2) followed by *in vitro* transcription using a MEGAscript kit (Ambion) as per the manufacturer's protocol. Transcription products were then electrophoresed onto a 6% PAGE containing 8 M urea, excised from the gel, then precipitated and after elution from the gel and ethanol. When necessary, purified RNA was dephosphorylated using CIP (New England Biolabs), 5′-end labelled with ATP γ-^{32}P (PerkinElmer) and T4 polynucleotide kinase (NE Biolabs), then treated with gel purification, passive elution and ethanol precipitation.

Structural analysis of RNAs

Structural analysis of end-labelled and gel-purified *csgD* mRNA or RydC was performed as described previously (4). Two pmol of 5′-end-labelled *csgD* mRNA was mixed with 100 pmol of cold RydC or 40 pmol of Hfq and incubated 30 or 10 min at 37°C, respectively. After the incubation, V_1 (5.10^{-5} or 15.10^{-5} U), S_1 (0.5, 1 or 2 U) or lead acetate (0.5 or 1 mM final) were added, and the mixes were incubated for 10 min more at 37°C. The reactions were precipitated and the pellets dissolved in loading buffer (Ambion). Samples were loaded onto an 8% PAGE containing 8 M urea. Gels were dried and visualized (Phosphor-Imager).

Hfq purification

Hfq was purified as previously described (4). *Escherichia coli* BL21(DE3) harbouring the pTE607 plasmid and grown at 37°C to an OD_{600} of 0.4. After induction with 1 mM Isopropyl β-D-1-thiogalactopyranoside (IPTG) during 3 h, cells were pelleted, dissolved in a buffer solution (20 mM Tris–HCL, 500 mM NaCl, 10% glycerol and 0.1% Triton X-100), sonicated, heated at 80°C for 10 min and finally centrifuged. Supernatant was then charged onto an 'AKTA purifier' (GE Healthcare) equipped with a Ni^{2+} column. Washes were performed with buffer containing 10 mM imidazole; the Hfq protein was eluted with the same buffer but with 300 mM imidazole. The purity of the protein was visualized on a 12% SDS–PAGE and concentration estimated by Bradford assay.

Toeprint and gel shift assays

After denaturation followed by renaturation at room temperature, annealing mixes containing 0.2 pmol *csgD mRNA* and 1 pmol of labelled primer were incubated for 15 min with or without various concentrations of RydC or Hfq. The fMet-tRNA^{fMet} was then added for 5 min. Reverse transcription was started by adding 2 µl of AMV RT (NE Biolabs) and dNTPs for 15 min and then stopped by adding 10 µl of Buffer II (Ambion). The cDNAs and sequencing reactions were run on polyacrylamide gels, and signals detected using a PhosphorImager. Gel retardation assays are performed as previously described (4). In all, 0.5 pmol of labelled RydC were incubated for 10 min at 37°C with various concentrations (0–500 pmols) of unlabelled *csgD* $mRNA_{215}$, *csgD* $mRNA_{\Delta 5'UTR}$ or *csgD* $mRNA_{100}$ in 1× Tris-$MgCl_2$-NaCl (TMN) buffer (20 mM Tris-acetate pH 7.6, 100 mM sodium acetate and 5 mM magnesium acetate). Samples were loaded onto a native 5% acrylamide gel and separated with 0.5× TBE at 4°C. Gels are dried and visualized (PhosphorImager).

In vitro translation assays

In vitro translation of CsgD $mRNA_{503}$ (2.5 pmols) using [^{35}S]-methionine was carried out with a PURESYSTEM (Cosmo Bio) following the manufacturer's instructions and as described previously (13). After RNA denaturation for 2 min at 85°C, chilling 2 min on ice and then renaturation for 5 min at 37°C in TMN 1× buffer, a pre-complex between RydC and 10 pmol of Hfq was performed during 10 min at 37°C. To form the complex with the *csgD* mRNA, we again incubated for 10 min at 37°C and then translation assays were initiated by adding [^{35}S]-methionine and the PURESYSTEM classic II. Each reaction was denatured in a 1× Laemmli buffer at 95°C for 5 min, loaded onto a 16% Tris-glycine gel and visualized on a PhosphorImager.

RESULTS

RydC induction reduces biofilm formation in two enteric bacteria

Bacterial sRNAs often regulate the expression of several targets (19). To search for a phenotype associated with the expression of RydC, *E. coli* strains either deficient in RydC

expression (*ΔRydC*) or harbouring a multicopy plasmid stimulating RydC expression was used. Interestingly, a 'RydC-dependent' biofilm phenotype was detected. After 48 h incubation at 28°C, in both *E. coli* and *S. enterica,* increasing RydC expression reduces biofilm formation by about one-third and one-half, respectively, when compared with isogenic strains (Figure 1A). The *ΔRydC E. coli* strain essentially forms biofilms in the same way the wild-type (wt) strain (Figure 1A). In the closely related *Shigella* genus, biofilm formation is impaired by mutations in the curli gene locus (20). Accordingly and irrespective of RydC, *S. sonnei* bacteria neither synthesize curli nor produce biofilms. Total RNAs were extracted from the biofilms and RydC levels were monitored by northern blots (Figure 1B). In the *E. coli* and *S. enterica* cells, RydC expression is low, probably after reduction by unknown factors to facilitate biofilm synthesis. This could explain the absence of phenotypic differences between the wt and *ΔrydC E. coli* strains. In the three enteric bacteria transformed with pUC-*rydC*, RydC induction was verified during biofilm formation (Figure 1B). It can be concluded that stimulation of RydC expression reduces biofilm formation in *E. coli* and *S. enterica.*

RydC lowers curli synthesis by reducing CsgA and CsgB protein and mRNA levels

In enteric bacteria, curli fibres are involved in surface adhesion, cell aggregation and biofilm formation (21). One possible explanation for the involvement of RydC in *E. coli* and *S. enterica* biofilm formation might be linked to curli biogenesis. Curliated bacteria stain red when grown on YESCA plates supplemented with Congo red diazo dye (22). After 48-h incubation at 28°C, stimulating RydC expression results in lowered curli formation in *E. coli* and *S. enterica* cells (Figure 2A). The Δ*rydC E. coli* strain forms consistently slightly more curli than isogenic cells (Figure 2A, right panel). During curli synthesis on YESCA plates with a RydC-overproducing strain, RydC gradually accumulates up to 15 h and remains high afterwards (Figure 2B). In *E. coli*, at least six proteins encoded by the *csgBA* and *csgDEFG* operons are dedicated to curli formation (22).

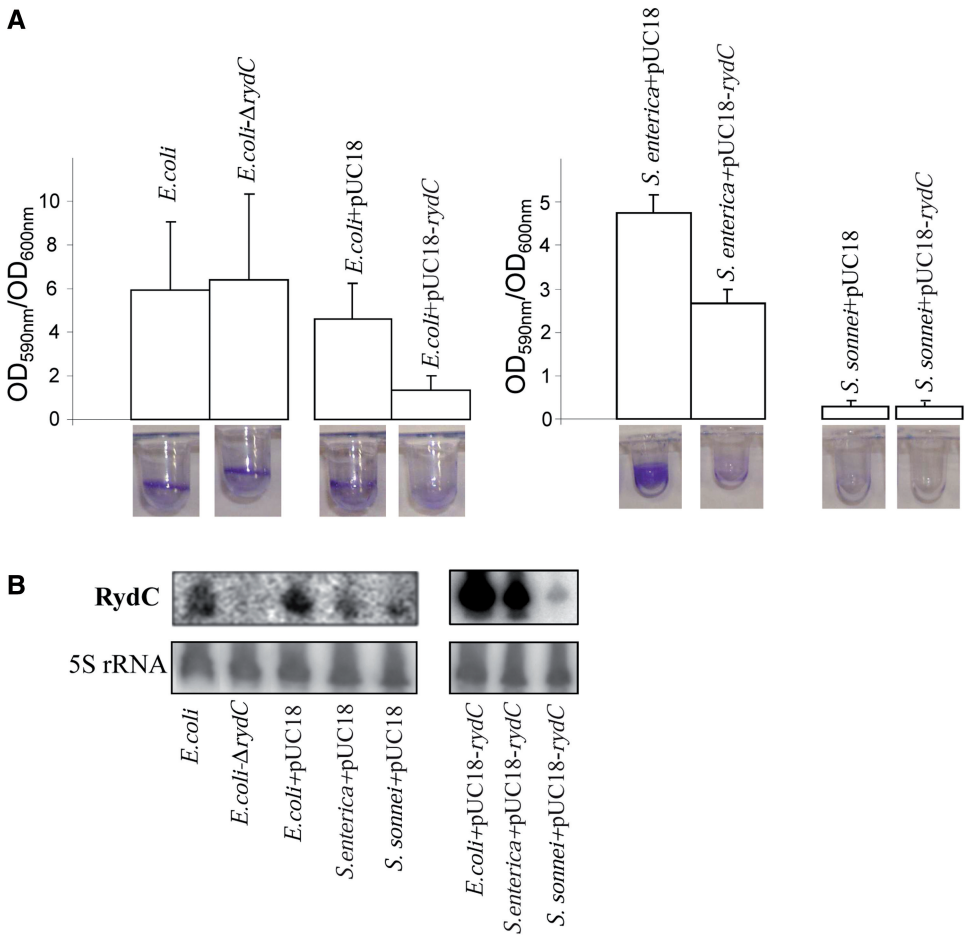

Figure 1. RydC regulates biofilm synthesis in *E. coli* and *S. enterica*. (**A**) Microtiter dish biofilm mass measured by crystal violet staining in *E. coli*, *S. enterica* (*bongori*) and *S. sonnei* after 48-h incubation. (left) The *E. coli* strains are wild-type MG1655Z1, its isogenic ΔRydC derivative (*ΔrydC*), strain containing a multicopy plasmid pUC18 and one containing pUC18 encoding RydC expressed from its endogenous promoter sequence (pUC18-*rydC*). (right) The same pUC18 constructs were added to *Salmonella* and *Shigella*. The data represent the means and standard deviations of at least 10 replicates. (**B**) RydC expression levels in the recombinant strains from the three bacteria monitored by northern blots on total RNAs directly extracted from the biofilms. The 5S rRNAs are internal loading controls.

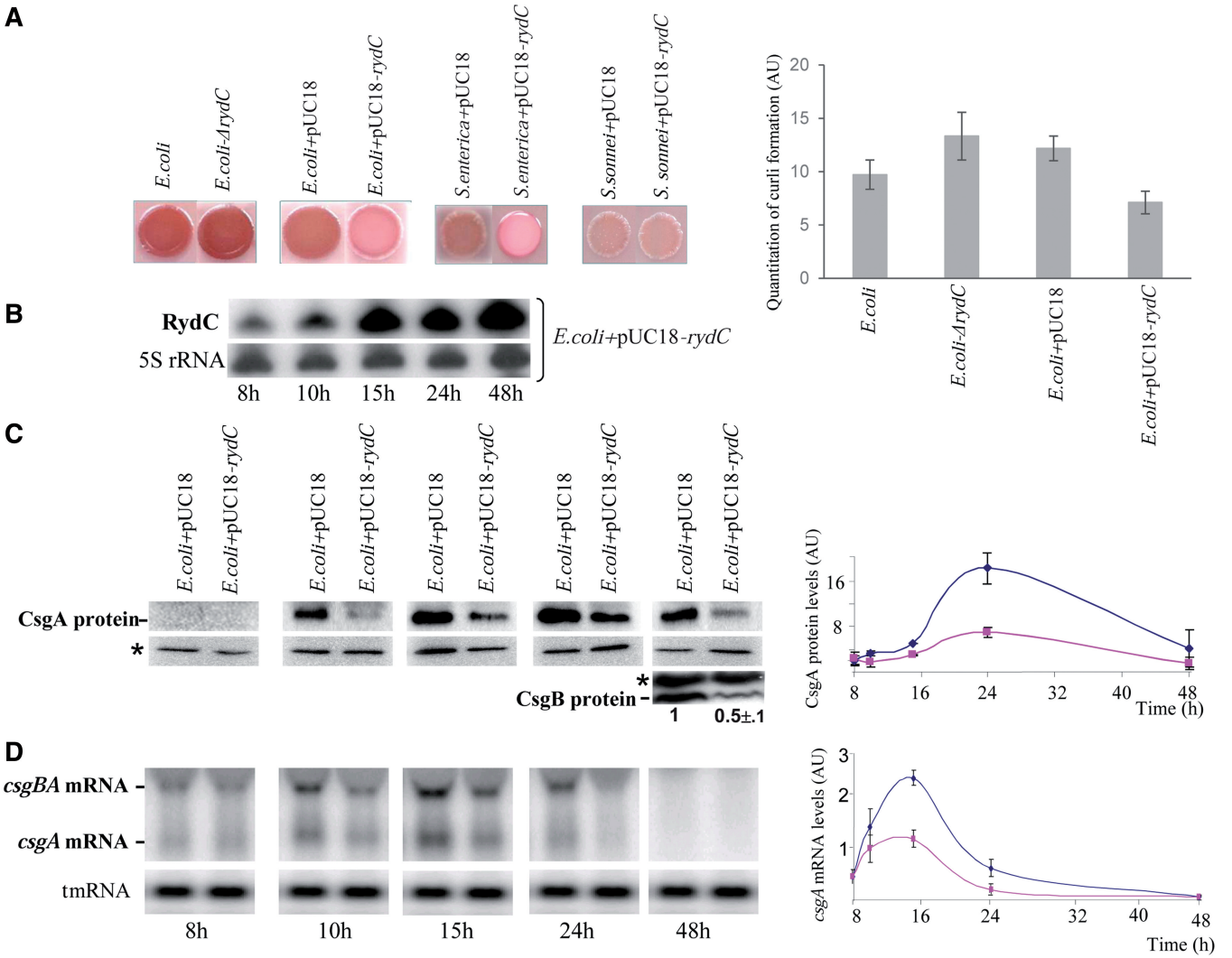

Figure 2. RydC induction lowers curli synthesis by reducing CsgA and CsgB protein and mRNA levels in enteric bacteria. (**A**) (left) Congo red (diazo dye) YESCA agar plates grown at 28°C for 48 h added to *E. coli*, *S. enterica* (*bongori*) and *S. sonnei*. The experiments were repeated at least three times. The *Shigella* strain does not form curli because its *csg* locus is disrupted by insertions and deletions (20), an action considered to be an internal negative control. (right) The graph shows quantitation of curli formation in the four isogenic strains using the GelQuant.NET software (Arbitrary Units, AU). The data are derived from three independent experiments. (**B**) Northern blots monitoring of 8–48 h of RydC expression in 'pUC18-*rydC*' isogenic strains, resulting in curli formations. As loading controls, the blots were also probed for 5S rRNA. (**C**) Immunoblots with anti-CsgA and anti-CsgB antibodies showing CsgA and CsgB protein expression in an *E. coli* strain harbouring pUC18-*rydC* versus an isogenic strain containing the empty plasmid (*E. coli* +pUC18). Curli formation was a result of 8–48-h of incubation on YESCA agar plates at 28°C for CsgA and 48 h for CsgB protein. The asterisks mark two aspecific protein bands, each revealed by one antibody. The graph shows CsgA protein quantification in the two isogenic strains (*E. coli*+pUC18 is blue; *E. coli*+pUC18-*rydC* is pink, Arbitrary Units, AU) relative to the levels of the aspecific protein. (**D**) Northern blot analysis of the *csgA* and *csgBA* mRNAs in the two strains during curli formation at identical time points, as in panel A. The blots were also probed for tmRNA as loading internal controls. The graph shows *csgA* mRNA quantification in the strains relative to tmRNA (using a similar colour code as panel C).

Homologous *agfBA* and *agfDEFG* operons were also identified in *Salmonella* (23). In *E. coli*, *csgBA* encodes the two curli structural subunits (24): CsgA is the major structural subunit, whereas CsgB is a nucleator. To determine whether RydC influences *csgBA* expression in *E. coli*, the effect of RydC accumulation on steady-state levels of the CsgA protein was monitored by western blots using anti-CsgA antibodies at several time points (0–48 h) during curli formation on YESCA plates. CsgA had a similar overall profile in a wt strain transformed with an empty vector as that of cells overexpressing RydC. CsgA is detected after 10-h incubation, increases up to 24 h and then decreases (Figure 2C). However, western blots show that stimulating RydC expression reduces the quantity of the CsgA structural protein by up to 2.5 times as compared with the wt (Figure 2C). After 24-h incubation, RydC induction strongly reduces CsgA levels. CsgB expression was also monitored after 48 h by western blots using anti-CsgB antibodies. Compared with an isogenic strain, promoting RydC expression also reduces the CsgB nucleator protein by about 2-fold (Figure 2C).

CsgA and CsgB proteins are produced from a single operon, and their RydC-induced reduction could originate from an mRNA-level regulation. Using a DNA probe targeting the *csgA* mRNA, two ~0.65- and ~1.15-kb-long transcripts were detected in the wt and RydC-overproducing strains by northern blots (Figure 2D), and these correspond, respectively, to the *csgA* and *csgBA* mRNAs (25). In the wt cells, the two mRNAs are detected early, and as expected their highest expression is around 15 h before optimal expression of the CsgA protein (Figure 2C), decreases thereafter, and is undetectable after 48 h (Figure 2D). During curli synthesis, after 10-h incubation high levels of RydC decrease the steady-state levels of *csgBA* and *csgA* mRNA transcripts by half. The stronger reduction of *csgBA* mRNA expression in the RydC-overproducing strain occurs after 15-h incubation. Thus, the maximum reduction of *csgBA* mRNA expression in the RydC-overexpressing strain occurs when RydC expression is highest (Figure 2B). In both strains, there is a 9 h interval between the peaks of *csgA* transcription and translation, which could be ascribed to unknown CsgA regulators acting at the post-transcriptional level. Additional time points between 15 and 24 h would be required to investigate this further. In summary, RydC induction impairs curli synthesis by lowering CsgA and B, mRNA and protein levels, in turn reducing biofilm formation.

RydC controls CsgD protein and mRNA expression levels

CsgD is a transcriptional activator of the *csgBA* operon required for curli and biofilm synthesis in *E. coli* (22). To assess whether RydC influences CsgD expression in *E. coli*, the effect of RydC expression on steady-state levels of the CsgD protein was monitored by western blots using anti-CsgD antibodies at several times during curli synthesis on YESCA plates (Figure 3A). CsgD protein expression was detected after 8-h incubation and increased to a maximum at 15 h, which as expected for a *csgBA* transcriptional activator corresponds to the peak of *csgBA* mRNA expression (Figure 2D), then slowly decreased down to zero after 48 h. This indicates that curli formation is substantially induced after 15-h incubation in *E coli*. Compared with an isogenic strain, at all times during curli synthesis, induction of RydC expression reduced the CsgD protein up to five-fold (Figure 3A). Thus, RydC impairs curli and biofilm synthesis by lowering CsgD protein levels. RydC may regulate CsgD expression at the mRNA level. During curli formation, RydC involvement in *csgD* mRNA levels was monitored by northern blots using a DNA probe specific for *csgD* mRNA. Hybridization of total RNAs extracted from curli-producing cells identified two ~0.9- and ~1.6-kb-long transcripts (Figure 3B), compatible, respectively, with the *csgD* and *csgDEF* mRNAs (22). The highest expression of the two mRNAs is at ~10 h and then it decreases to nothing after 48 h (Figure 3B). During curli formation, the *csgD* mRNA and protein expressions peak before that of *csgBA* mRNA and proteins, which is as expected for a transcriptional regulator when compared with its target genes. Throughout curli synthesis, inducing RydC expression reduces the *csgD* mRNA steady-state levels down to half when compared with the isogenic strain. There is about a 5 h gap between the peaks of *csgD* transcription and translation that might be ascribed to previously reported or unknown regulators of csgD expression acting at the post-transcriptional level. Additional time points between 10 and 15 h would be required to further investigate this observation. Compared with an isogenic strain, the lack of endogenous levels of RydC increases *csgD* mRNA synthesis about three-fold after 8 h of curli formation on YESCA plates (Figure 3C). This result demonstrates the negative influence of RydC on *csgD* mRNA steady-state levels *in vivo*. RydC reduces biofilm formation by impairing curli synthesis through lowering of CsgD protein and mRNA levels, in turn decreasing *CsgA* mRNA and CsgA and *CsgB* protein levels.

CsgD expression reduction by RydC interaction with csgD mRNA and the influence of the mRNA 5′-UTR in complex formation

RydC controls *csgD* mRNA expression either indirectly via dedicated regulators or directly by antisense pairings with the mRNA. The *CsgDEFG* mRNA transcriptional start site was mapped by primer extension analysis and is located 146 nt upstream from the CsgD initiation codon (22). Gel retardation assays were used to analyse duplex formation between RydC and a 215 nt-long *csgD* mRNA fragment ($mRNA_{215}$). The $mRNA_{215}$ contains the 5′-UTR sequence (146 nt) followed by 69 nt corresponding to the first 23 codons from its coding sequence (Figure 4A). An 'RydC-*csgD* $mRNA_{215}$' duplex was detected (Figure 4B and Supplementary Figure S1) and its binding is specific, as a 100-fold molar excess of unrelated RNA (SprD) does not remove the *csgD* $mRNA_{215}$ from its preformed 'RydC–*csgD* $mRNA_{215}$' complex. To test the importance of the *csgD* mRNA 5′-UTR in the binding of RydC, a *csgD* mRNA deletion mutant lacking the 5′-UTR and starting at G_{+3} was constructed ($mRNA_{\Delta 5'UTR}$). The $mRNA_{\Delta 5'\text{-}UTR}$ does not interact with RydC (Figure 4B), demonstrating that the *csgD* mRNA 5′-UTR is essential for binding. Is the entire 5′-UTR of *csgD* mRNA required? To see if this is so, a second mutant ($mRNA_{100}$) was made containing 31 nt from the *csgD* mRNA 5′-UTR including the TIS, followed by 69 nt from its coding sequence. A 'RydC-*csgD* $mRNA_{100}$' duplex was detected (Figure 4B and Supplementary Figure S1), and the binding was specific, as a 100-fold molar excess of unrelated RNA (SprD) did not remove the *csgD* $mRNA_{100}$ from its preformed 'RydC–*csgD* $mRNA_{100}$' complex. The binding ability of $mRNA_{100}$ with RydC was lower than that with $mRNA_{215}$ (Figure 4B and Supplmentary Figure S1), suggesting structural differences between these mRNAs (see later in the text), or a lower affinity between RydC and $mRNA_{100}$ as compared with that of $mRNA_{215}$. Our results demonstrate that RydC forms a stable complex with the *csgD* mRNA *in vitro* and that at least a section of its 5′-UTR, including the TIS, is required for binding.

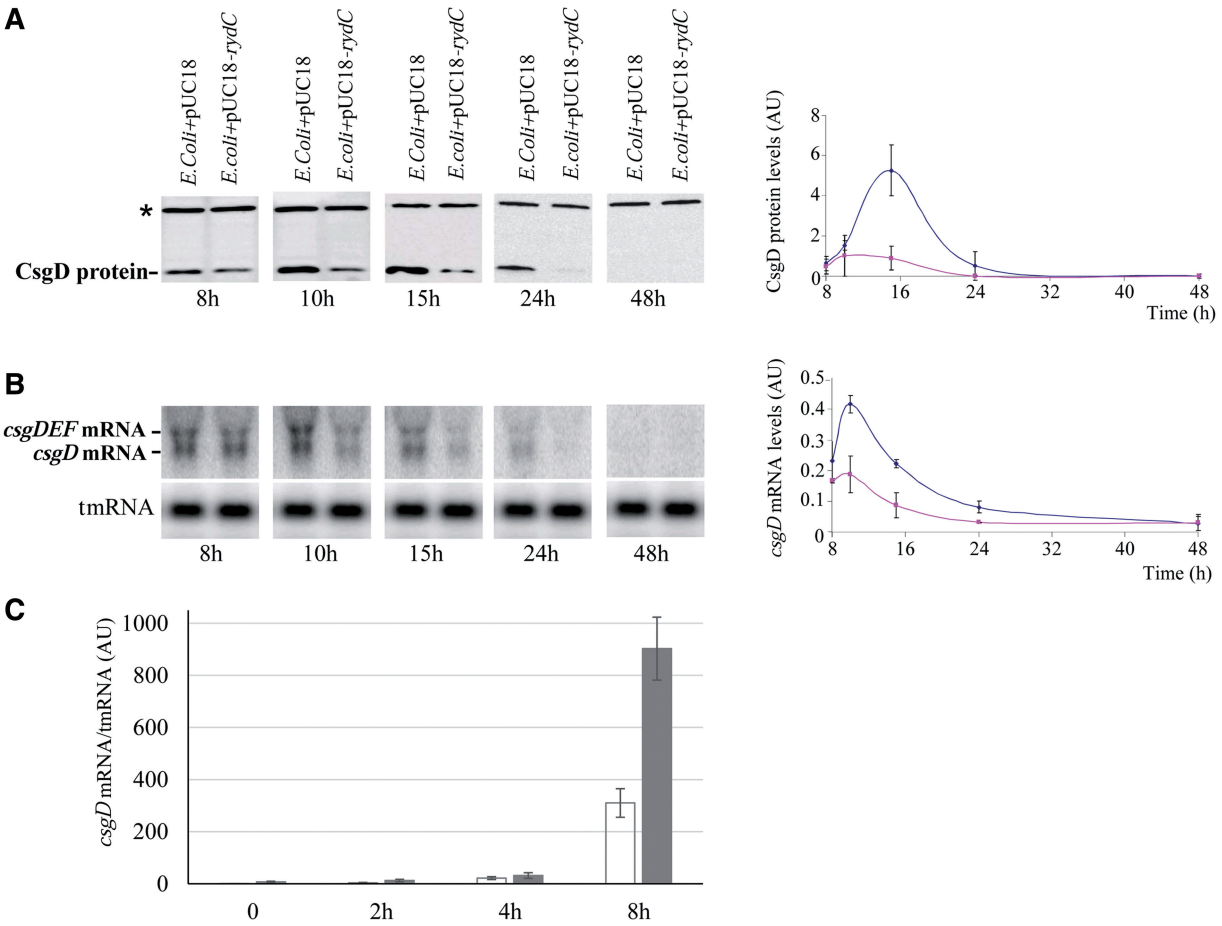

Figure 3. RydC lowers *csgD* mRNA and protein levels and the absence of endogenous levels of RydC increases *csgD* mRNA synthesis during curli formation. (**A**) Immunoblots with anti-CsgD antibodies monitoring CsgD protein expression between 8 to 48 h curli formation on YESCA agar plates at 28°C in an *E. coli* strain harbouring pUC18-*rydC* versus an isogenic strain containing the empty plasmid (*E. coli*+pUC18). The asterisk indicates an aspecific protein revealed by the antibody. The graph shows CsgD protein quantification in the two isogenic strains (*E. coli*+pUC18 is blue; *E. coli*+pUC18-*rydC* is pink, Arbitrary Units, AU) relative to the amount of the aspecific protein. (**B**) Northern blot analysis of the *csgD* and *csgDEF* mRNAs in the two strains during curli formation at time points, as in panel A. The blots were also probed for tmRNA as loading internal controls. The graph shows *csgD* mRNA quantification in the strains relative to tmRNA (similar colour code as in panel A, Arbitrary Units, AU). (**C**) The qPCR comparison of *csgD* mRNA expression in *E. coli* (white) and *E. coli-ΔrydC* (dark grey) strains during curli formation for 8 h on YESCA plates, normalized against the *tmrna* reference gene (Arbitrary Units, AU). The downregulation of *csgD* mRNA by RydC occurs after 4 h of incubation.

Hfq facilitates the interaction between RydC and the csgD mRNA

RydC interacts with Hfq *in vitro,* and the protein considerably enhances RydC stability *in vivo* (4). Therefore, Hfq may facilitate the pairings between RydC and *csgD* mRNA. To test this, gel retardation assays were performed between labelled RydC, purified *E. coli* Hfq (1:1 molar ratio relative to RydC) and increasing concentrations of unlabelled *csgD* $mRNA_{215}$. An 'RydC–Hfq–*csgD* $mRNA_{215}$' ternary complex is detected (Figure 4C, left), and nearly all of the RydC is in the complex at a one-to-one molar ratio with *csgD* $mRNA_{215}$. In the absence of Hfq, to obtain about half the amount of RydC in complex with its target, there is a need for a 1000-fold molar excess of *csgD* $mRNA_{215}$ versus RydC (Supplementary Figure S1). This also indicates that RydC and *csgD* $mRNA_{215}$ can simultaneously interact with Hfq. In the absence of RydC, Hfq interacts with the *csgD* $mRNA_{215}$ *in vitro* (Figure 4C, right). Hfq facilitates the interaction between RydC and the *csgD* mRNA, improving the efficiency of the regulation.

The csgD mRNA ribosome binding site is sequestered by RydC and by Hfq to prevent translation initiation

Because the interaction of RydC with the *csgD* mRNA requires the 31 nt upstream from the initiation codon that contain the TIS, RydC could prevent ribosome loading onto the *csgD* mRNA. To test this, toeprint assays were performed on ternary initiation complexes, including purified ribosomes, initiator $tRNA^{fMet}$ and the *csgD* $mRNA_{215}$. A strong ribosome toeprint was detected at position C_{+15} on *csgD* $mRNA_{215}$, 14 nt downstream from A_{+1} of the initiation codon (Figure 5A, left). Minor toeprints were also detected upstream, at positions A_{+22} and A_{+26}, suggesting some degree of freedom in the

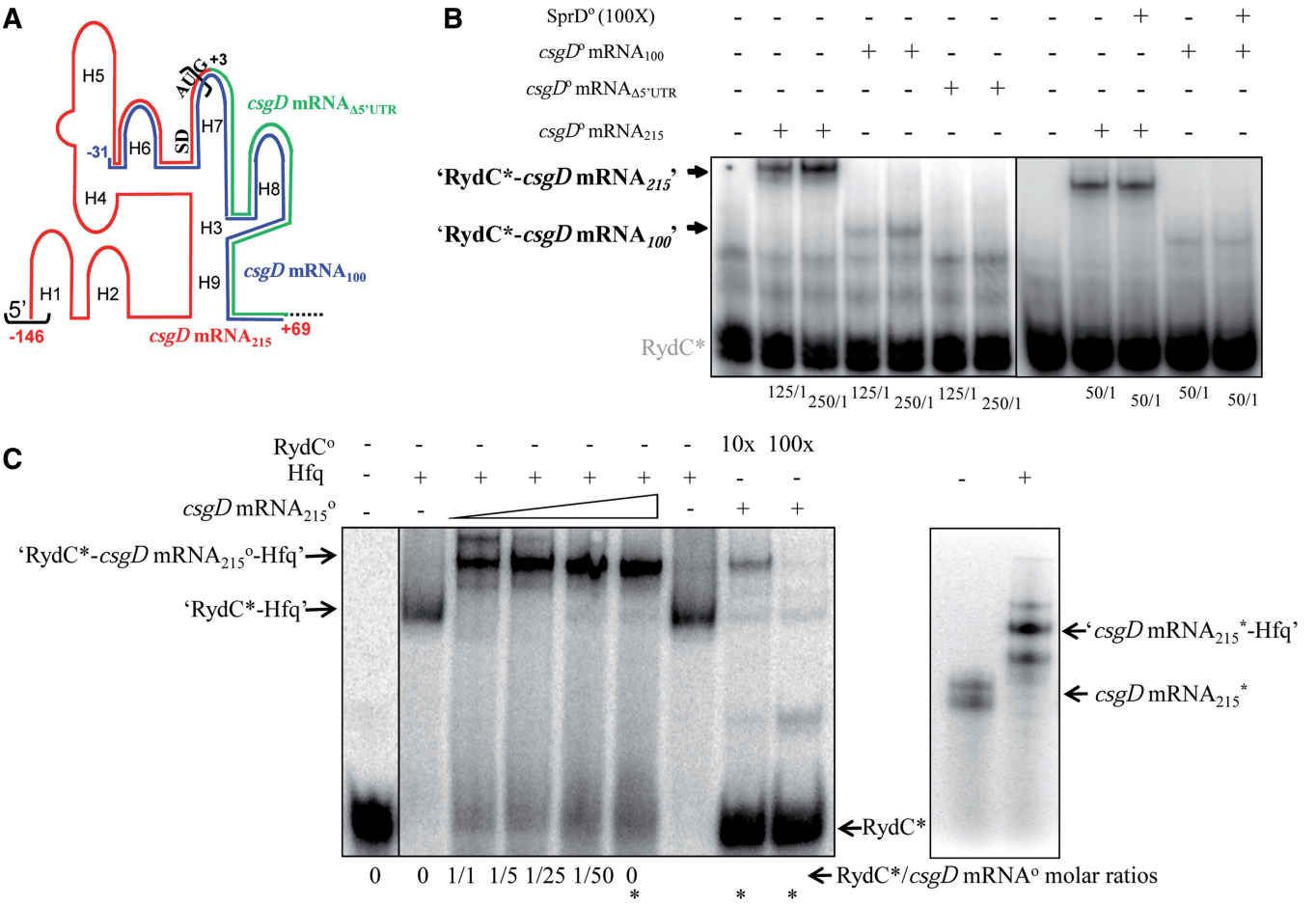

Figure 4. Direct interaction between RydC and the *csgD* mRNA; ternary complex formation between RydC Hfq and its mRNA target. (**A**) Schematic representation of the *csgD* mRNA 5′-domain emphasizing three RNA constructs. The *csgD* $mRNA_{215}$ corresponds to the 215 nt from the 5′-end of the mRNA (red), emphasizing the SD and AUG translation initiation signals. In the *csgD* $mRNA_{100}$ variant (blue), 115 nt from the *csgD* mRNA 5′-end were deleted. The 5′-UTR of the *csgD* mRNA (the sequence between the black brackets) was deleted in mutant *csgD* $mRNA_{\Delta 5'\text{-}UTR}$, therefore starting at G_{+3} (green). (**B**) Complex formation between RydC and each of the three *csgD* mRNA constructs. Native gel retardation assays of purified labelled RydC with increasing amounts of purified unlabelled *csgD* $mRNA_{215}$, *csgD* $mRNA_{100}$ or *csgD* $mRNA_{\Delta 5'\text{-}UTR}$ are shown. The *csgD* mRNA construct/RydC molar ratios are indicated below each lane. Competition assays were performed with a 100-fold molar excess of unrelated purified SprD RNA (18) in the presence of each of the *csgD* $mRNA_{215}$ and *csgD* $mRNA_{100}$ constructs. (**C**) Ternary complex formation between RydC, *csgD* $mRNA_{215}$ and Hfq. Left panel: Native gel retardation assays show complex formation between labelled RydC and increasing amounts of unlabelled *csgD* $mRNA_{215}$ (at a 1- to 50-fold excess as compared with RydC) in the presence or absence of purified Hfq. Hfq is at a 1:1 molar ratio with RydC. The asterisks indicate the 'RydC*/*csgD* mRNA' molar ratio used to perform the competition assays with a 10- to 100-fold molar excess of unlabelled RydC. Right panel: *csgD* $mRNA_{215}$ interacts with Hfq in the absence of RydC *in vitro*. Hfq is at a 20:1 molar ratio with the mRNA. The *csgD* mRNA adopts two conformations on a native gel.

positioning of the ribosome onto *csgD* $mRNA_{215}$, or else a structural rearrangement of the mRNA on ribosome binding. In the absence of Hfq, RydC reduced ribosome loading onto the *csgD* mRNA in a concentration-dependent manner, requiring elevated amounts of sRNA for the regulation (Figure 5A, left). In the absence of RydC, low amounts of purified Hfq also prevent *csgD* mRNA translation initiation (Figure 5A, right). Thus, both Hfq alone or elevated amounts of RydC have the ability to reduce CsgD translation initiation *in vitro*.

Monitoring the CsgD mRNA conformation by structural probes

As a prerequisite, conformations of free *csgD* $mRNA_{215}$ and free *csgD* $mRNA_{100}$ were investigated in solution. Both transcripts were end labelled and their solution structures were probed by RNase V_1, which cleaves double-stranded RNAs or stacked nucleotides, and by nuclease S_1 and lead, which both cleave accessible single-stranded RNAs. The reactivity towards these structural probes was monitored for each nucleotide (Supplementary Figure S2 for *csgD* $mRNA_{215}$ and Supplementary Figure S3 for *csgD* $mRNA_{100}$). The data are summarized onto the supporting model of *csgD* $mRNA_{215}$ (Figure 6A) and csgD $mRNA_{100}$ (Supplementary Figure S3). For *csgD* $mRNA_{215}$, the data showed the existence of nine folded helices (H1–H9, with V_1 cuts and without lead or S1 cleavages), all of which except H3 and H9 are capped by loops (presenting S_1 and lead cleavages but no V_1 cuts). An internal bulge between H4 and H5 was revealed by numerous S_1 cuts at G_{-62}-U_{-65}. Structural analysis of the *csgD* mRNA is consistent with a previous RNase T_1 and lead analysis (13) that proposed the existence of SL1 (H4–H5) and SL2 (H7). However, our data suggest the

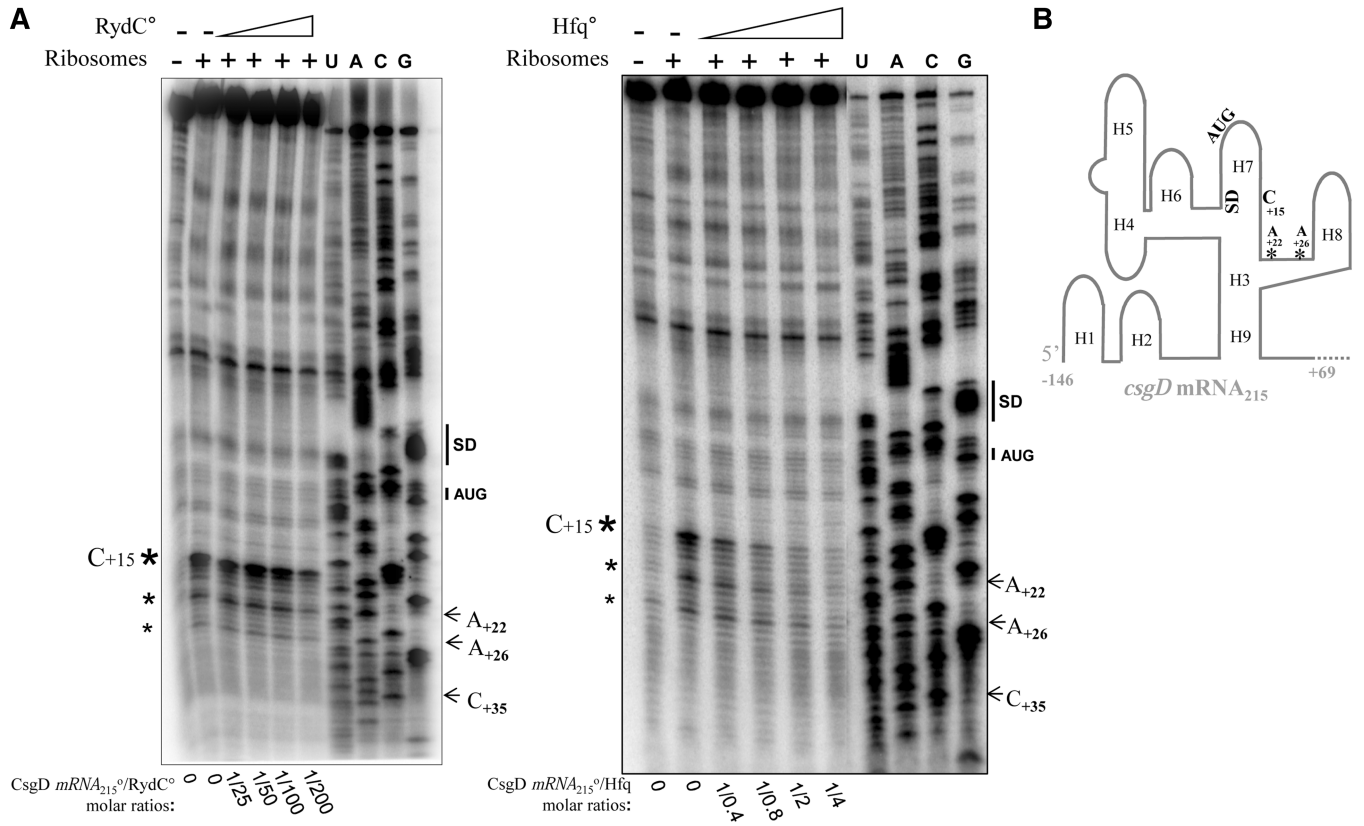

Figure 5. Hfq and RydC both prevent ribosome loading onto the *csgD* mRNA. (**A**) Ribosome toeprint assays performed on *csgD* $mRNA_{215}$ in the presence of increasing amounts of RydC or purified Hfq. Left panel: 25- to 200-fold excess RydC as compared with *csgD* $mRNA_{215}$. Right panel: 0.4- to 4-fold excess purified Hfq as compared with *csgD* $mRNA_{215}$. The experimentally proven toeprints are indicated with asterisks, with their sizes reflecting the intensity of the toeprints. Plus/minus indicates the presence of purified ribosomes with the *csgD mRNA*; U, A, G and C: indications of the *csgD* $mRNA_{215}$ sequencing ladders. The SD sequence and AUG initiation codon of the *csgD* $mRNA_{215}$ are also indicated. (**B**) Schematic representation of the *csgD mRNA* 5′-domain, emphasizing the location of the ribosome toeprints (marked with asterisks) induced by either Hfq or RydC.

existence of additional helices (H1–H3, H6, H8–H9; Figure 6A) that may not be conserved (13). Probing data indicate that the beginning of the *csgD* mRNA coding sequence is tightly folded and embedded within four helices (H3, H7–H9). The conformation of *csgD* $mRNA_{100}$ was monitored by structural probes (Supplementary Figure S3), and these data were compatible with the existence of H7 and H8. In that shorter mRNA fragment, however, the conformation of its 5′- and 3′-ends is different than that of *csgD* $mRNA_{215}$: it lacks H6 and H9 but has an additional helix (H10) that bridges the 5′- and 3′-ends (Supplementary Figure S3). H7, H8 and H10 are joined by three accessible single-stranded RNAs (U_{-25}-A_{-14}, A_{+22}-A_{+26} and C_{+50}-U_{+60}).

Monitoring the 'RydC–CsgD mRNA' complex by structural probes

Structural changes induced by RydC complex formation were examined by subjecting the 'RydC–*csgD* $mRNA_{215}$' and 'RydC–*csgD* $mRNA_{100}$' complexes to nuclease S_1, RNases V_1 and lead statistical digestions. Binding of RydC induced a cluster of structural changes located in a similar restricted region within the two *csgD* mRNA constructs encompassing the SD and AUG sequences, from A_{-20} to G_{+3} (Figure 6A, Supplementary Figures S2 and S3). When RydC interacts with *csgD* $mRNA_{215}$, the sRNA pseudoknot undergoes structural changes at its 5′-end that includes S1, H1 and L1 (Figure 6B and Supplementary Figure S2), as a result of which S1 and L1 should become double stranded. The structural data support a model of interaction between *csgD* mRNA and RydC in which 'L6-H7-L7' from the mRNA (including the TIS) pairs with 'S1-H1-L1' from RydC (Figure 6C). To provide additional experimental evidence for the proposed pairing model, a *csgD* mRNA mutant lacking H6–H9 was engineered and produced (*csgD* $mRNA_{115}$, Figure 6D). Based on the probing data and pairing model, it should not be able to bind RydC. When *csgD* $mRNA_{215}$ was in complex with RydC, there was no structural modifications at the first 115 nt from the *csgD* mRNA 5′-end (Figure 6A and Supplementary Figure S2). *CsgD* $mRNA_{115}$ did not interact with RydC, even when at a 250-fold excess (Figure 6D), indicating that the recognition domains of *csgD* mRNA for binding RydC are not in the first 115 nt from the mRNA leader region. Conversely, a RydC mutant lacking 'S1-H1-L1' was constructed ($RydC_{\Delta 5'}$, Figure 6E), and gel retardation assays with *csgD* $mRNA_{215}$ revealed the absence of complex formation between the two RNAs (Figure 6E, right). Translation assays provide direct experimental evidence that, unlike wt RydC, $RydC_{\Delta 5'}$ was unable to reduce *csgD* mRNA translation (Figure 6E, right).

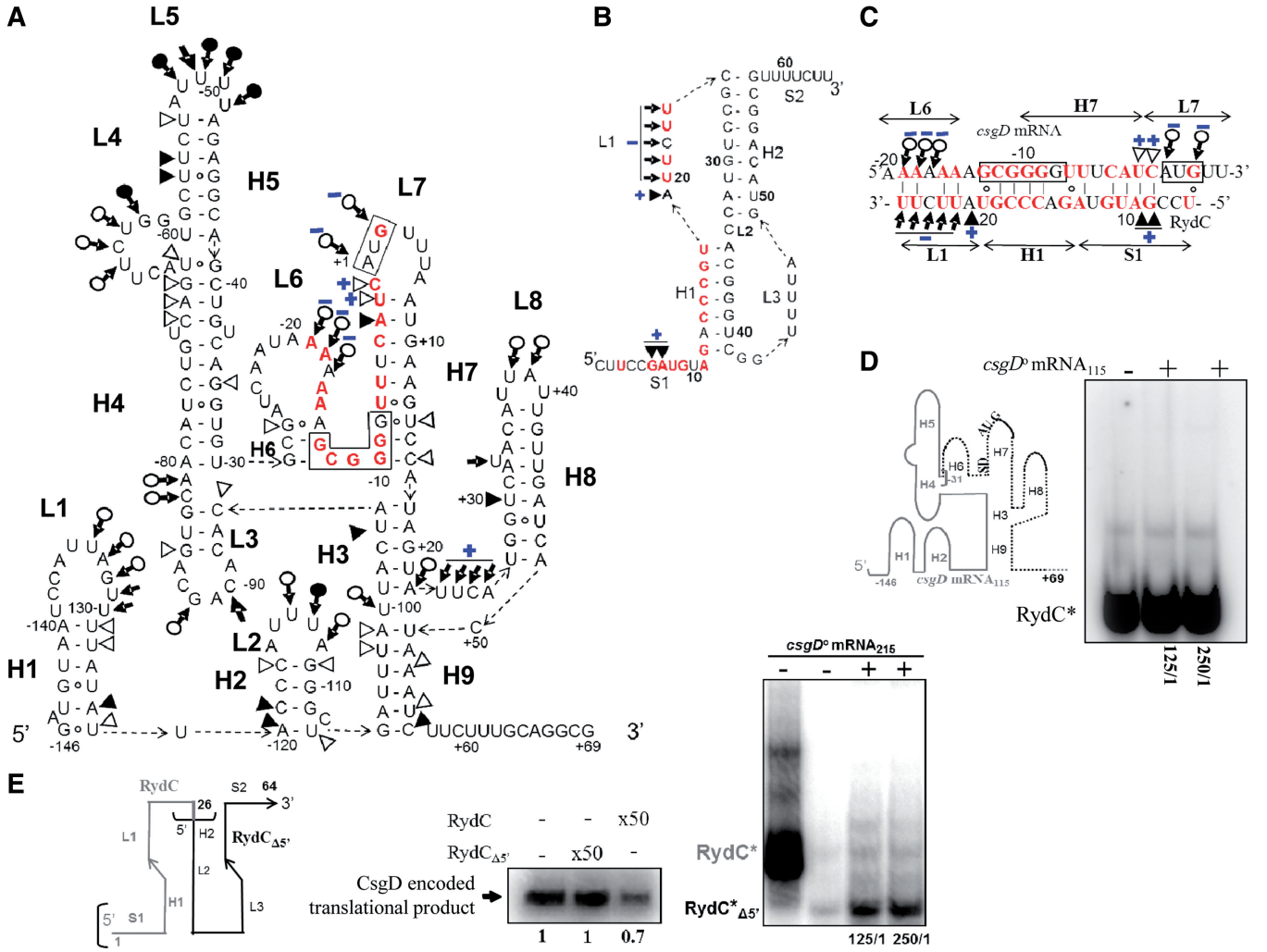

Figure 6. Structural probing and deletion analysis of the interaction between RydC and *csgD* mRNA. (**A**) Secondary structure of the *csgD* $mRNA_{215}$ 5′-end (−146 to +69 nt) from *E. coli*. This is based on structural probes in solution (Supplementary Figure S2), which provide experimental support for the proposed structure. Triangles are V_1 cuts; arrows capped by a circle are S_1 cuts; plain arrows are lead cleavages. Cleavage intensity is shown with filled (strong cuts) or open (weaker) symbols. Structural domains (H1–H9, L1–L8) are indicated. The structural changes in the *csgD* mRNA induced by RydC are blue. Most of these changes are clustered onto L6-H6 and H7-L7. Nucleotides from the *csgD* mRNA proposed to interact with RydC are in red (for details, see Figure 7). (**B**) RydC secondary structure (4) emphasizing the nucleotides from its 5′-domain (red) interacting with the *csgD* mRNA. The structure is based on probing (Supplementary Figure S3) and mutational analysis (panel E and Figure 7). Structural changes induced by the binding of *csgD* mRNA with RydC are clustered on S1-H1-L1. Only the structural changes induced by duplex formation are indicated here, using the same indicators as in section A. (**C**) Proposed antisense pairing between RydC and the *csgD* mRNA leads to the sequestration of the mRNA ribosome binding site (outlined) by the RydC 5′-domain. Pairing interactions between RydC and the *csgD* mRNA are based on native gel retardation assays, deletion analysis and structural mapping of RydC in complex with the *csgD* mRNA. Only the structural data concerning the RNA duplex conformation is indicated, with the same symbols and colours as Figure 6A. The blue plus (+) and minus (−) signs indicate the appearance or disappearance of cleavages induced by structural probes when the two RNAs are, respectively, in duplex (**D**). RydC binding does not require 115 nt from the *csgD* mRNA 5′-end. Schematic representation of the *csgD* mRNA 5′-domain, emphasizing the *csgD* $mRNA_{115}$ construct (in grey), which lacks the H6–H9 domains (dotted lines). The grey bracket delineates the shorter *csgD* $mRNA_{115}$ construct. Native gel retardation assays of purified labelled RydC with increasing amounts of *csgD* $mRNA_{115}$ (125- to 250-fold excess relative to RydC) show that the first 115 nt from the *csgD* mRNA 5′-end are unable to interact with RydC. This result is in agreement with the probing data, which reveal a lack of structural changes in this area of the mRNA when in complex with RydC. (**E**) Native gel retardation and *in vitro* translation evidence that the RydC 5-domain interacts with and controls CsgD translation. Left panel: Schematic representation of RydC, emphasizing the $RydC_{\Delta 5'}$ construct (in black), which lacks the S1-H1-L1 5′-domains (in grey). Right panels: a 250-fold excess of synthetic purified $RydC_{\Delta 5'}$ is unable to bind with *csgD* $mRNA_{215}$, whereas wild-type RydC can (Figure 4B). *In vitro* translation of *csgD* $mRNA_{215}$ in the presence of $RydC_{\Delta 5'}$ at a 50-fold molar ratio with the *csgD* mRNA, showing that the RydC 5′-domain S1-H1-L1 is essential in lowering CsgD translation. The lack of $RydC_{\Delta 5'}$ activity is due to its incapacity to interact with the *csgD* mRNA, as evidenced by the absence of complex formation (upper panel).

Hfq induces a conformational rearrangement of the csgD mRNA

Structural changes induced by complex formation between Hfq and the *csgD* mRNA were examined by subjecting an 'Hfq-*csgD* $mRNA_{215}$' complex to nuclease S_1, RNases V_1 and lead statistical digestions (Supplementary Figure S4). Binding of Hfq induced a cluster of structural changes on the *csgD* mRNA at loops L4, L4-5, L5 and L6, all of which became protected

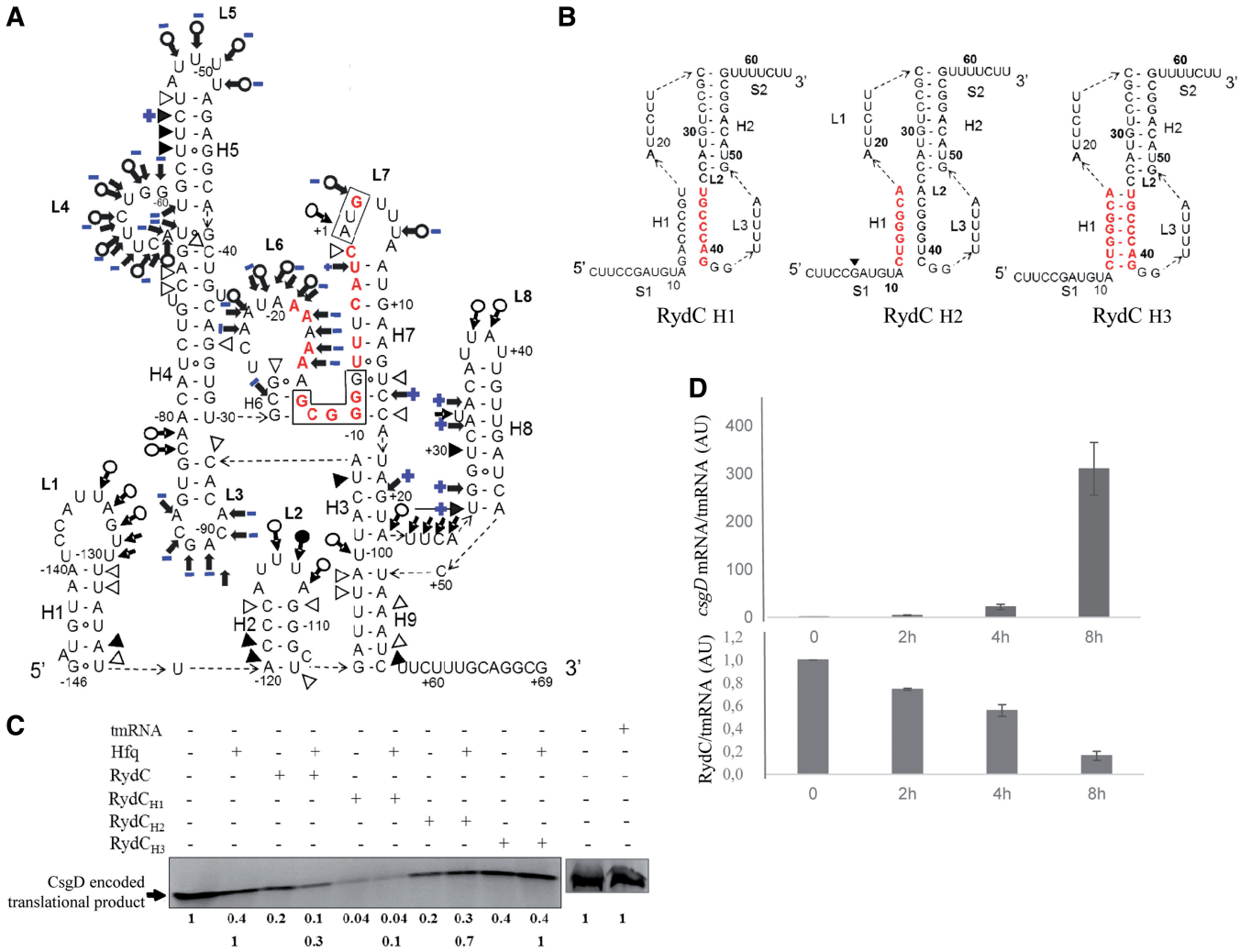

Figure 7. The interaction between Hfq and *csgD* mRNA, the role of Hfq in translational regulation and the inverse correlation between RydC and *csgD* mRNA expression during curli formation *in vivo*. (**A**) Secondary structure of *csgD* mRNA$_{215}$, with the structural changes induced by Hfq on the *csgD* mRNA conformation in blue. This model is based on structural probing of the RNA-protein complex in solution (Supplementary Figure S4). The blue plus (+) and minus (−) signs indicate the appearance or disappearance of cleavages induced by the structural probes when the protein is in complex with the mRNA. (**B**). RydC mutants with mutated nucleotides in red: disrupted stem H1 (RydC$_{H1}$), stem H1 and the interacting sequence with the *csgD* mRNA (RydC$_{H2}$) and a compensatory mutant that restores the H1 structure (RydC$_{H3}$). (**C**) *In vitro* translation of *csgD* mRNA$_{503}$ in the presence of various RydC mutants, with and without a 2-fold molar excess of Hfq. The translation products arbitrarily set to 1 were quantified relative to *csgD* mRNA$_{503}$ translation in the absence of RydC and Hfq (upper lane). To explore the effect of RydC in the presence of Hfq, the translation products were also set to 1 and quantified relative to CsgD translation in the presence of Hfq (lower lane); tmRNA was used as an internal negative control. (**D**) qPCR monitoring of *csgD* mRNA and RydC expression in *E. coli* cells during curli formation on YESCA plates, normalized against the *tmrna* reference gene.

against lead and S_1 cuts (Figure 7A and Supplemenary Figure S4). This provides direct evidence for structural modifications of the *csgD* mRNA 5′-UTR. Hfq also induced reactivity changes within the *csgD* mRNA coding sequence, especially within helices H7 and H8 (Figure 7A). This indicates that Hfq induced a significant conformational rearrangement of the *csgD* mRNA 5′-UTR, including part of its actual coding sequence.

Evaluation of the involvement of the RydC structure and pairings in regulation of csgD mRNA translation

According to the probing data and the RNA deletion mutants (Figure 6), one can predict that the RydC domains S1-H1-L1 will interact with the *csgD* mRNA. Specific mutations were generated within the central element of the pairing interaction, stem H1 (Figure 7). These disrupted the pseudoknot fold (RydC$_{H1}$), removed its *csgD* mRNA binding site (RydC$_{H2}$) or restored stem H1 (RydC$_{H3}$). Mutant RydC$_{H1}$ disrupts stem H1 and therefore unfolds the pseudoknot while maintaining its *csgD* mRNA binding site, resulting in increased efficacy and translation blockage in the absence of Hfq (Figure 7C). This shows that unfolding the RydC pseudoknot greatly enhances its translational control of *csgD* mRNA. Mutant RydC$_{H2}$ had a similar effect on CsgD translation, implying that pairings between S1, L1 and the *csgD* mRNA TIS are necessary and sufficient for

translational control. In the regulation triggered by $RydC_{H2}$, in which the pseudoknot was unfolded, the addition of Hfq was not beneficial. Finally, compensatory mutant $RydC_{H3}$ was only half as active as RydC in reducing *csgD* mRNA translation, and Hfq had no effect on the translation regulation induced by $RydC_{H3}$. Because $RydC_{H3}$ is ~10-fold less active than $RydC_{H1}$ for reducing CsgD translation, it suggests that an unfolded state of the RydC pseudoknot significantly increases its capacity to reduce CsgD translation.

RydC and Hfq control of csgD mRNA translation

In vitro translation assays were done to provide direct experimental evidence that RydC, Hfq or 'RydC–Hfq' complex represses *csgD* mRNA protein synthesis. These assays were performed on a *csgD* $mRNA_{503}$ construct encoding the first 119 amino acids of the CsgD protein. Without RydC and Hfq, a 13-kDa polypeptide was detected (Figure 7C). Hfq reduced CsgD translation down to 40%. This is in agreement with the substantial reduction of the ribosome toeprints induced by Hfq (Figure 5A, right), and the 20% reduction of translation by RydC (Figure 7C). When RydC and Hfq acted together, CsgD translation dropped down to 10%. Hfq or elevated amounts of RydC by themselves reduced CsgD translation by impairing ribosome binding, but the presence of an 'Hfq–RydC' complex significantly amplified the regulation. As an internal negative control, similar concentrations of tmRNA did not impact CsgD translation when compared with RydC (Figure 7C), demonstrating the specificity of the RydC-induced CsgD translation reduction.

DISCUSSION

In this report, we show that RydC expression affects biofilm formation and cell adhesion in two enterobacteria: *S. enterica* and *E. coli*. RydC is an important negative regulator of curli synthesis *in vivo*, as its endogenous expression gradually decreases over time while *csgD* mRNA expression progressively increases and triggers curli synthesis and biofilm formation (Figure 7D). In addition, the lack of endogenous levels of RydC augments *csgD* mRNA synthesis (Figure 3C). This tiny 64 nt-long sRNA also regulates the expression of a membrane transporter involved in nutrient and antibiotic uptake (5,6). *Escherichia coli* RydC possesses at least two direct targets (*yejABEF* and *csgD* mRNAs), which suggests physiological links between these encoded proteins. In *Salmonella*, RydC regulates bacterial membrane integrity through mRNA stabilization of cyclopropane fatty acid synthase (8). Thus, RydC acts both as a target activator/repressor and as a sensor for nutrient uptake, membrane remodelling and biofilm formation (Figure 8A). Interestingly, the RydC pairings with both *cfa* and *csgD* mRNAs involve accessible nucleotides at the RydC 5′-end, although in the case of the *csgD* mRNA, the pairing interaction is longer and spreads deeper into the sRNA pseudoknot. When food supplies are available and enter the bacteria, RydC expression is turned on to enable nutrient uptake and membrane stabilization. It also prevents unwanted biofilm formation, avoiding this survival mode triggered in hostile environments such as under feeding limitations. Previous observations (4) are in agreement with our conclusions, as RydC expression is activated during the exponential growth phase and 'switched off' at the stationary phase. However, when enteric bacteria are in 'curli' and 'biofilm' modes, RydC expression gradually decreases over time (Figure 7D), probably due to unknown regulators. RydC-induced reduction of biofilm formation and cell adhesion results from a drop-off in curli synthesis via the direct downregulation of CsgD expression at both the RNA and protein levels, which in turn lowers CsgA and CsgB curli structural proteins levels. The *csgD* mRNA is a direct target of RydC and Hfq, reducing translation initiation by blocking the mRNA TIS through direct pairings.

In *E. coli*, RydC is the sixth Hfq-dependent sRNA that negatively controls CsgD transcription factor expression, and all of these sRNAs impair translation initiation. With the help of Hfq, OmrA, OmrB, RprA, McaS, GcvB and RydC regulate CsgD expression by pairing at the *csgD* mRNA 5′-UTR (13–17). Each of these six possesses specific binding sites on the *csgD* 5′-UTR, some with binding overlaps (Figure 8B). Interestingly, most of the structural changes induced by Hfq on the *csgD* mRNA overlap with the binding sites of these sRNA regulators (Figure 8B). Hfq modifies the conformation of the *csgD* mRNA at and around the binding sites of each of these sRNAs, probably to facilitate pairing between the mRNA target and its RNA regulators. Hfq can, however, repress *csgD* mRNA translation in the absence of sRNA, as recently observed in the translation inhibition of the *cirA* mRNA involved in iron uptake (26).

Interestingly, RydC is the only sRNA from the group that pairs exclusively at the *csgD* mRNA TIS rather than upstream (RprA interacts at both the TIS and upstream). In fact, RydC binding still occurred after the removal of 115 nt at the *csgD* mRNA 5′-end (Figure 4). In addition, RydC reduces cellular levels of *csgD* mRNA (Figure 3), implying that the regulation occurs at both the post-transcriptional and translational levels, as is usually the case for 'Hfq-dependent' sRNAs (27). In bacteria, transcription and translation are simultaneous, but we detected ~5-h delay between *csgD* mRNA and protein synthesis (Figure 3). This is attributable to previously reported or unknown regulators of csgD expression acting at the post-transcriptional level. As reported for other sRNAs that interact with Hfq, RydC-Hfq-induced CsgD translation inhibition could promote target mRNA turnover, stimulating endonucleolytic cleavages and decay (28).

The *CsgD* 5′-UTR structure, inferred from structural probes, is highly folded and includes a portion of the TIS (Figure 6A). This implies unfolding both when translation initiates and when initiation is blocked through the joint action of Hfq and the six sRNAs that bind at various locations within the *csgD* 5′-UTR (Figure 8B). In this latter situation, each sRNA acts as a specific external stimulus sensor (Figure 8A). Hfq facilitates interactions between an sRNA and its targets by binding both RNAs or by restructuring one or both RNAs (3). We previously

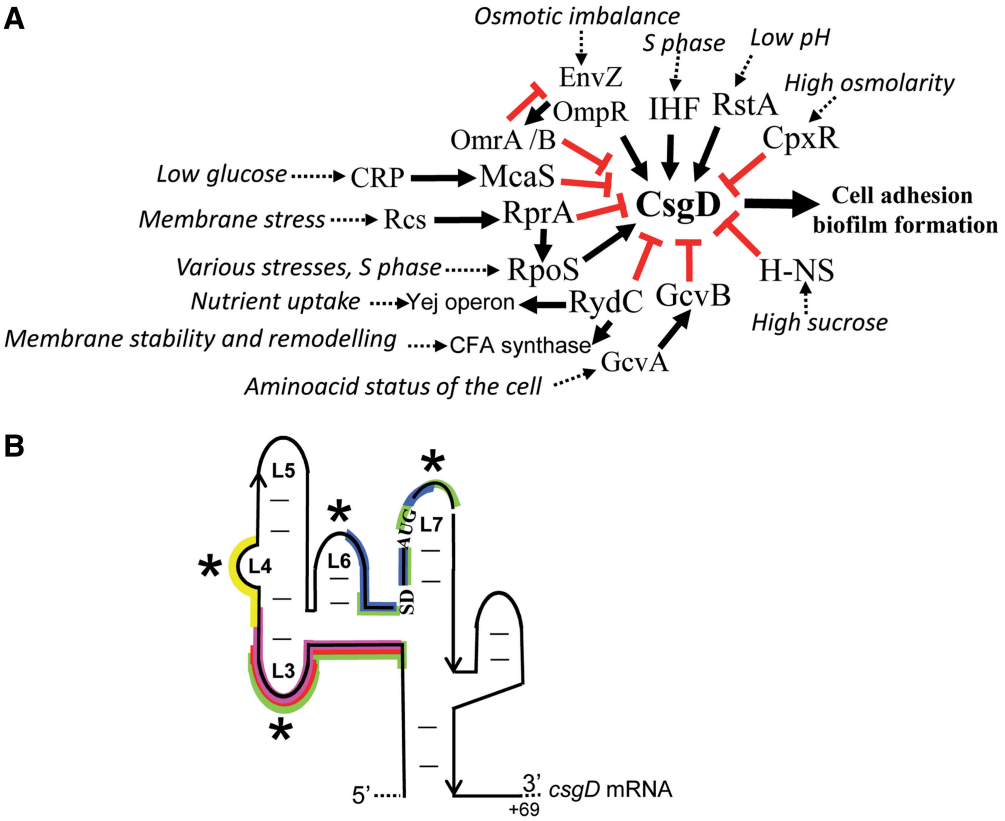

Figure 8. Schematic integration of protein and RNA regulators of CsgD expression, colocalization of the binding sites of the six sRNAs regulating this expression and the Hfq-induced mRNA structural changes. (**A**) The proteins and sRNAs (16) that control CsgD expression in response to various specific environmental changes that trigger cell adhesion and biofilm formation. The black arrows and red bars indicate positive and negative regulations, respectively. Endogenous levels of RydC induce positive regulations of the Yej operon (4) and of CFA synthase expression (8). The various environmental triggers that influence and initiate these regulations are in italics, the ultimate effector molecule being the CsgD transcription factor. (**B**) The binding sites of the six sRNAs that reduce CsgD translation initiation are indicated on the *csgD* mRNA 5′ platform. OmrA/B is yellow, GcvB is pink, McaS is red, RprA is green and RydC is blue. The asterisks indicate the *csgD* mRNA domains from that are subjected to reactivity changes in the presence of Hfq, which strikingly match the sRNA binding sites.

reported that Hfq binds RydC and restructures its conformation (4), presumably to facilitate pairing with its mRNA targets. Based on previous probing data collected on a RydC–Hfq complex (4), the protein induces reactivity changes at the two connecting single-stranded loops within the RydC pseudoknot, triggering pairing rearrangements within H1. Hfq modifies RydC structure, thus destabilizing H1 (4) but also changing *csgD* mRNA conformations. These particular RydC domains are those with which our structural and mutational evidence indicates *csgD* mRNA interacts. Hfq interacts with *csgD* mRNA (Figure 4C) and reduces its translation in the absence of sRNAs (Figure 5A). As previously reported for *sodB* mRNA (28), Hfq remodels both the conformations of RydC and *csgD* mRNA to improve translational control. In the absence of Hfq, the ribosomal toeprint on the *csgD* mRNA requires a large amount of RydC (Figure 5A). Accordingly, CsgD translation decreases only when RydC is in excess (Figure 7C). Interestingly, RydC is considerably lowered in the presence of Hfq. This implies that Hfq is required *in vivo* to regulate RydC-induced *csgD* translation initiation. Hfq orientation and proximity to the complementary target site may facilitate RydC unfolding and the annealing between the two RNAs (29). Hfq could also assist in the exchange of RNA strands between the interacting RNAs.

For the most part, single strands accessible within the scaffolds of sRNAs pair with their mRNA targets, occasionally requiring conformational activations. The interaction between RydC and *csgD* mRNA is striking because it is the first time that an interaction between an mRNA target and an sRNA pseudoknot, which requires chaperone-induced restricted unfolding, is reported. These observations come from structural and mutational analysis of 'sRNA-mRNA' duplexes, which indicate that the RydC 5′-end is involved in pairings with the *csgD* mRNA TIS. For pairing, helices H1 from RydC and H7 from the *csgD* mRNA should unfold. This is probably facilitated by Hfq, which interacts with both RydC (4) and *csgD* mRNA, to form a ternary complex with the two RNAs (Figure 4). The 5′-seeding between RydC 5′-accessible nucleotides and the *csgD* mRNA AUG codon is involved in pairing. Demonstrated previously by probing (4), RydC pseudoknot 'breathing' in solution opens helix H1 to promote pairing with the *csgD* mRNA, a transition facilitated by Hfq.

Pseudoknots are ingenious dynamic structural modules that can be temporarily unfolded (here with the assistance of a chaperone) to allow for antisense seed pairing and subsequent propagation. Two pseudoknots have already been detected and experimentally validated in another bacterial sRNA (29). In that case, they both contained an internal open reading frame that can only be translated under specific conditions. Bacterial sRNAs can act as anti-toxic components in toxin–antitoxin systems, and an RNA pseudoknot was recently reported to inhibit and antagonize a harmful protein in the toxin–antitoxin pair (30). Antisense RNAs can modulate mRNA pseudoknot formation to control plasmid replication (31), indicating that pseudoknot structural plasticity can also be manipulated by chaperoned RNAs to control gene expression. In addition to their essential roles as *cis*-regulatory modules within mRNAs (31), including riboswitches (32), regulatory sRNAs pseudoknots are, when assisted by RNA chaperones, ingenious tools for efficient and reversible gene regulation processes in living organisms.

SUPPLEMENTARY DATA

Supplementary Data are available at NAR Online.

ACKNOWLEDGEMENTS

The authors are thankful to Prof. M. Chapman (University of Michigan) for the gift of the polyclonal antibodies to CsgA and CsgB, to Dr Hajnsdorf (IBPC, Paris) for providing plasmid pTE607 plasmid for Hfq expression and purification, to Dr M. Guillier (IBPC, Paris) and Dr M. Hallier (our laboratory) for critical reading of the manuscript and comments and to Dr S. Chabelskaya and A. Eyraud from our laboratory for providing SprD and purified ribosomes, respectively.

FUNDING

Agence Nationale pour la Recherche [ANR-09-MIEN-030-01 to B.F.]; Institut National de la Santé Et de la Recherche Médicale (INSERM); Ministère de l'Enseignement supérieur et de la Recherche. Funding for open access charge: INSERM.

Conflict of interest statement. None declared.

REFERENCES

1. Storz,G., Vogel,J. and Wassarman,K.M. (2011) Regulation by small RNAs in bacteria: expanding frontiers. *Mol. Cell*, **43**, 880–891.
2. Sobrero,P. and Valverde,C. (2012) The bacterial protein Hfq: much more than a mere RNA-binding factor. *Crit. Rev. Microbiol.*, **38**, 276–299.
3. Soper,T.J., Doxzen,K. and Woodson,S.A. (2011) Major role for mRNA binding and restructuring in sRNA recruitment by Hfq. *RNA*, **17**, 1544–1550.
4. Antal,M., Bordeau,V., Douchin,V. and Felden,B. (2005) A small bacterial RNA regulates a putative ABC transporter. *J. Biol. Chem.*, **280**, 7901–7908.
5. Novikova,M., Metlitskaya,A., Datsenko,K., Kazakov,T., Kazakov,A., Wanner,B. and Severinov,K. (2007) The *Escherichia coli* Yej transporter is required for the uptake of translation inhibitor microcin C. *J. Bacteriol.*, **189**, 8361–8365.
6. Eswarappa,S.M., Panguluri,K.K., Hensel,M. and Chakravortty,D. (2008) The yejABEF operon of *Salmonella* confers resistance to antimicrobial peptides and contributes to its virulence. *Microbiology*, **154**, 666–678.
7. Ortega,A.D., Gonzalo-Asensio,J. and Garcia-del Portillo,F. (2012) Dynamics of *Salmonella* small RNA expression in non-growing bacteria located inside eukaryotic cells. *RNA Biol.*, **9**, 469–488.
8. Frohlich,K.S., Papenfort,K., Fekete,A. and Vogel,J. (2013) A small RNA activates CFA synthase by isoform-specific mRNA stabilization. *EMBO J.*, **32**, 2963–2979.
9. Hall-Stoodley,L., Costerton,J.W. and Stoodley,P. (2004) Bacterial biofilms: from the natural environment to infectious diseases. *Nat. Rev. Microbiol.*, **2**, 95–108.
10. Romling,U. (2005) Characterization of the rdar morphotype, a multicellular behaviour in *Enterobacteriaceae*. *Cell Mol. Life Sci.*, **62**, 1234–1246.
11. Ogasawara,H., Yamada,K., Kori,A., Yamamoto,K. and Ishihama,A. (2010) Regulation of the *Escherichia coli* csgD promoter: interplay between five transcription factors. *Microbiology*, **156**, 2470–2483.
12. Pesavento,C., Becker,G., Sommerfeldt,N., Possling,A., Tschowri,N., Mehlis,A. and Hengge,R. (2008) Inverse regulatory coordination of motility and curli-mediated adhesion in *Escherichia coli*. *Genes Dev.*, **22**, 2434–2446.
13. Holmqvist,E., Reimegard,J., Sterk,M., Grantcharova,N., Romling,U. and Wagner,E.G. (2010) Two antisense RNAs target the transcriptional regulator CsgD to inhibit curli synthesis. *EMBO J.*, **29**, 1840–1850.
14. Thomason,M.K., Fontaine,F., De Lay,N. and Storz,G. (2012) A small RNA that regulates motility and biofilm formation in response to changes in nutrient availability in *Escherichia coli*. *Mol. Microbiol.*, **84**, 17–35.
15. Mika,F., Busse,S., Possling,A., Berkholz,J., Tschowri,N., Sommerfeldt,N., Pruteanu,M. and Hengge,R. (2012) Targeting of csgD by the small regulatory RNA RprA links stationary phase, biofilm formation and cell envelope stress in *Escherichia coli*. *Mol. Microbiol.*, **84**, 51–65.
16. Jorgensen,M.G., Nielsen,J.S., Boysen,A., Franch,T., Moller-Jensen,J. and Valentin-Hansen,P. (2012) Small regulatory RNAs control the multi-cellular adhesive lifestyle of *Escherichia coli*. *Mol. Microbiol.*, **84**, 36–50.
17. Boehm,A. and Vogel,J. (2012) The csgD mRNA as a hub for signal integration via multiple small RNAs. *Mol. Microbiol.*, **84**, 1–5.
18. Kikuchi,T., Mizunoe,Y., Takade,A., Naito,S. and Yoshida,S. (2005) Curli fibers are required for development of biofilm architecture in *Escherichia coli* K-12 and enhance bacterial adherence to human uroepithelial cells. *Microbiol. Immunol.*, **49**, 875–884.
19. Wagner,E.G., Altuvia,S. and Romby,P. (2002) Antisense RNAs in bacteria and their genetic elements. *Adv. Genet.*, **46**, 361–398.
20. Sakellaris,H., Hannink,N.K., Rajakumar,K., Bulach,D., Hunt,M., Sasakawa,C. and Adler,B. (2000) Curli loci of Shigella spp. *Infect. Immun.*, **68**, 3780–3783.
21. Barnhart,M.M. and Chapman,M.R. (2006) Curli biogenesis and function. *Annu. Rev. Microbiol.*, **60**, 131–147.
22. Hammar,M., Arnqvist,A., Bian,Z., Olsen,A. and Normark,S. (1995) Expression of two csg operons is required for production of fibronectin- and congo red-binding curli polymers in *Escherichia coli* K-12. *Mol. Microbiol.*, **18**, 661–670.
23. Collinson,S.K., Clouthier,S.C., Doran,J.L., Banser,P.A. and Kay,W.W. (1996) *Salmonella enteritidis* agfBAC operon encoding thin, aggregative fimbriae. *J. Bacteriol.*, **178**, 662–667.
24. Hammar,M., Bian,Z. and Normark,S. (1996) Nucleator-dependent intercellular assembly of adhesive curli organelles in *Escherichia coli*. *Proc. Natl Acad. Sci. USA*, **93**, 6562–6566.
25. Arnqvist,A., Olsen,A. and Normark,S. (1994) Sigma S-dependent growth-phase induction of the csgBA promoter in *Escherichia coli* can be achieved *in vivo* by sigma 70 in the absence of the nucleoid-associated protein H-NS. *Mol. Microbiol.*, **13**, 1021–1032.

26. Salvail,H., Caron,M.P., Belanger,J. and Masse,E. (2013) Antagonistic functions between the RNA chaperone Hfq and an sRNA regulate sensitivity to the antibiotic colicin. *EMBO J.*, **32**, 2764–2778.
27. Gottesman,S. and Storz,G. (2011) Bacterial small RNA regulators: versatile roles and rapidly evolving variations. *Cold Spring Harb. Perspect. Biol.*, **3**, pii: a003798.
28. Aiba,H. (2007) Mechanism of RNA silencing by Hfq-binding small RNAs. *Curr. Opin. Microbiol.*, **10**, 134–139.
29. Panja,S. and Woodson,S.A. (2012) Hfq proximity and orientation controls RNA annealing. *Nucleic Acids Res.*, **40**, 8690–8697.
30. Sayed,N., Jousselin,A. and Felden,B. (2012) A cis-antisense RNA acts in trans in *Staphylococcus aureus* to control translation of a human cytolytic peptide. *Nat. Struct. Mol. Biol.*, **19**, 105–112.
31. Brantl,S. (2007) Regulatory mechanisms employed by cis-encoded antisense RNAs. *Curr. Opin. Microbiol.*, **10**, 102–109.
32. Babitzke,P., Baker,C.S. and Romeo,T. (2009) Regulation of translation initiation by RNA binding proteins. *Annu. Rev. Microbiol.*, **63**, 27–44.